

## GT2007-27238 D - R - A - F - T

### SCATTERING AND GENERATION OF ACOUSTIC ENERGY BY A PREMIX SWIRL BURNER

**Alexander Gentemann**  
ASKON Consulting GmbH  
D-80333 München  
Germany

**Wolfgang Polifke\***  
Lehrstuhl für Thermodynamik  
Technische Universität München  
D-85747 Garching  
Germany  
polifke@td.mw.tum.de

#### ABSTRACT

*The scattering and generation of acoustic energy by a pre-mix swirl burner is scrutinized. The analysis is formulated in terms of the scattering matrix of the burner, determined by a combination of computational fluid dynamics and system identification as well as experiment supplemented with simple analytical models for flame frequency response and burner transfer matrix.*

*Remarkably, it is found that in a narrow range of frequencies, incoming acoustic waves are amplified strongly by the unsteady heat release, i.e. acoustic energy is generated. Although the computational and experimental data were obtained for one specific swirl burner design, the analysis suggests that such behavior should be common for many burner designs. Consequences for thermo-acoustic stability as well as burner and combustor design strategies are discussed.*

#### INTRODUCTION

In recent years, more stringent NO<sub>x</sub>-emission regulations have been a driving force for gas turbine development, leading to the wide-spread introduction of the lean pre-mix combustion technology. Operational experience has shown that lean pre-mix combustion is susceptible to self-excited thermo-acoustic instabilities, leading to limited operability or even structural damage. Clearly, combustion oscillations need to be considered and if

possible eliminated early in the design process, and not during commissioning.

Interactions between acoustics and heat release are often described in terms of a flame frequency response  $F(\omega)$

$$F(\omega) \equiv \frac{\dot{Q}'/\dot{Q}}{u'_B/u_B}, \quad (1)$$

where  $\dot{Q}'$  are fluctuations of the overall rate of heat release, and  $u_B$  is the flow velocity at the burner mouth, say. More general<sup>1</sup>, the burner transfer matrix  $\mathbf{T}$  relates fluctuation amplitudes of pressure  $p'(\omega)$  and velocity  $u'(\omega)$  upstream (subscript  $u$ ) and downstream (subscript  $d$ ) of the burner

$$\begin{pmatrix} \frac{p'}{\rho c} \\ u' \end{pmatrix}_d \equiv \mathbf{T}(\omega) \cdot \begin{pmatrix} \frac{p'}{\rho c} \\ u' \end{pmatrix}_u. \quad (2)$$

In the limit of plane-wave linear acoustics, the transfer matrix  $\mathbf{T}$  provides a complete description of the acoustic behavior of a flame or a burner (generally speaking, of an "acoustic element" or "multi-port"). By combining individual transfer matrices, so-called *network models* are obtained [1]. This computationally efficient "low-order" method has been successfully adapted to

<sup>1</sup>Under certain conditions, it is possible to deduce the transfer matrix of a flame from its frequency response  $F$  (see below).

\*Address all correspondence to this author.

the study of self-excited combustion instabilities by many researchers, e.g. [2–5].

Unfortunately, knowledge of the frequency response  $F(\omega)$  or the transfer matrix  $\mathbf{T}(\omega)$  of a burner are in general not sufficient to assess the stability properties of a combustor. In addition the impedance  $Z(\omega) \equiv p'/u'$  at the location of heat release must be known, which depends on the acoustic wave field – and therefore also on the acoustic boundary conditions – of the combustion system. Once the impedance is known, the *Rayleigh index*

$$RI \equiv \oint p' \dot{Q}' dt \quad (3)$$

can be determined. The famous *Rayleigh criterion* then states that self-excited instability *may* occur if  $RI > 0$ , because in that case the phase-correlated fluctuations of pressure and heat release feed energy into the oscillation. A positive Rayleigh index does not mean that instability *must* occur, because losses of acoustic energy (e.g. at the system boundaries) may outweigh the generation at the flame.

Although the Rayleigh criterion is ubiquitous in the literature on combustion instabilities, it is very rarely evaluated explicitly in stability analysis, with the recent exceptions of publications by Nicoud et al. and Ibrahim et al. [6, 7]. The authors propose to assess system stability by evaluating the sources and sinks of acoustic energy and then balancing them against each other.

In this context it is obviously of interest to scrutinize the scattering of acoustic energy at a burner. This is the topic of the present paper: Starting from the transfer matrix  $\mathbf{T}$  or the flame frequency response  $F$ , amplification factors  $\Pi$  for acoustic energy are introduced. Given an acoustic wave impinging on the burner, an amplification factor  $\Pi > 1$  indicates that the acoustic energy flux of outgoing waves – be it reflected or transmitted components – is larger than the ingoing energy flux, i.e. acoustic energy is generated by the interaction of acoustics and heat release. Analyzing experimental and numerical data for a pre-mix swirl burner, amplification factors  $\Pi$  much larger than unity are found in a narrow range of frequencies. Consequences for thermo-acoustic stability as well as burner and combustor design strategies are discussed.

## SCATTERING MATRIX

Mathematically equivalent to Eq. (2) is a formulation which makes use of *characteristic wave amplitudes*

$$f \equiv \frac{1}{2} \left( \frac{p'}{\bar{\rho}c} + u' \right) \text{ and } g \equiv \frac{1}{2} \left( \frac{p'}{\bar{\rho}c} - u' \right), \quad (4)$$

travelling in the downstream and the upstream direction, respectively, and a *scattering matrix*  $\mathbf{S}(\omega)$  such that across an acoustic

element

$$\begin{pmatrix} f_d \\ g_u \end{pmatrix} \equiv \mathbf{S} \cdot \begin{pmatrix} f_u \\ g_d \end{pmatrix}, \quad (5)$$

The characteristic wave amplitudes  $(f_u, g_d)$  on the r.h.s of this equation represent the waves incident on the multi-port, while  $(f_d, g_u)$  on the l.h.s. represent emitted waves. The coefficients of the scattering matrix may be identified as transmission and reflection coefficients  $T$  and  $R$  of the waves  $f_u$  and  $g_d$  incident from the up- and the downstream direction, respectively:

$$\mathbf{S} = \begin{pmatrix} T_u & R_d \\ R_u & T_d \end{pmatrix}. \quad (6)$$

Transfer and scattering matrix can be converted into each other by linear algebraic operations, e.g.

$$S_{11} = 2(\mathbf{T}_{11}\mathbf{T}_{22} - \mathbf{T}_{12}\mathbf{T}_{21})/\Omega \quad (7)$$

$$S_{12} = (\mathbf{T}_{11} - \mathbf{T}_{12} + \mathbf{T}_{21} - \mathbf{T}_{22})/\Omega \quad (8)$$

$$S_{21} = (-\mathbf{T}_{11} - \mathbf{T}_{12} + \mathbf{T}_{21} + \mathbf{T}_{22})/\Omega \quad (9)$$

$$S_{22} = 2/\Omega, \quad (10)$$

$$\text{with } \Omega \equiv \mathbf{T}_{11} - \mathbf{T}_{12} - \mathbf{T}_{21} + \mathbf{T}_{22}, \quad (11)$$

and similarly for the conversion from  $\mathbf{S}$  to  $\mathbf{T}$ .

## Determination of Scattering Matrices from CFD and System Identification

For simple geometries, transfer matrices (and equivalently scattering matrices) may be derived from the (linearized) equations of conservation of mass and momentum and suitable additional assumptions [2, 4, 5, 8]. However, in general the determination of the matrix coefficients from first principles is not possible, and one has to resort to experiment or numerical simulation. Experience has shown that the former requires very careful experimental work – especially in the presence of turbulent flow or combustion – sophisticated post-processing of large amounts of raw data, and long test runs, if the transfer matrix is to be recorded accurately over a range of frequencies [9, 10].

It therefore appears attractive to determine the transfer matrix of an acoustic element from numerical simulation. The idea is to carry out a time-dependent computational fluid dynamics (CFD) simulation of the compressible flow through the multi-port and reconstruct or *identify* the matrix coefficients from the time series data generated in this manner. System behavior – and in particular system stability – is investigated again with the network model, making use of a combination of transfer matrices obtained from first principles as well as experiment or simulation..

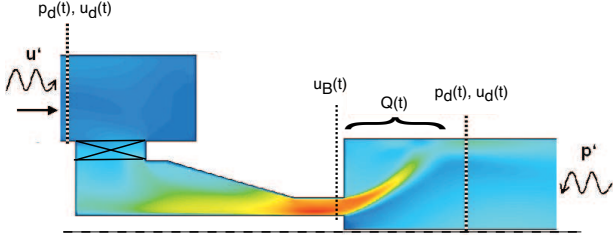


Figure 1. SCHEMATIC OF CFD/SI SETUP FOR IDENTIFICATION OF TRANSFER MATRIX OF A PREMIX SWIRL BURNER AS WELL AS FREQUENCY RESPONSE OF FLAME. PRESSURE AND VELOCITY ARE EXPORTED AT SAMPLING PLANES UPSTREAM ( $u$ ) AND DOWNSTREAM ( $d$ ) OF THE BURNER AS WELL AS AT THE BURNER MOUTH ( $B$ ). OVERALL RATE OF HEAT RELEASE  $\dot{Q}(t)$  IS OBTAINED AS A VOLUME INTEGRAL OVER HEAT RELEASE DENSITY.

This approach has been developed by Polifke et al. [11–14], inspired by earlier work on the determination of flame frequency responses from CFD [3, 15–17]. The procedure, which we shall refer to as CFD/SI in the following, combines stationary CFD simulation with *correlation analysis*, as it is known from system identification (SI): A CFD simulation with broad-band excitation of flow variables at the boundaries of the computational domain generates time series of fluctuating pressure  $p(t)$  and velocity  $u(t)$  at sampling planes located up- and downstream of the element to be identified (a swirl burner in the case at hand, c.f. Fig. 1). From the time series obtained, the auto-correlation matrix  $\Gamma$  of incoming acoustic signals  $f_u$  and  $g_d$  as well as the cross-correlation vector  $\vec{c}$  of incoming and outgoing acoustic signals are estimated. Inversion of the *Wiener-Hopf equation*

$$\Gamma \cdot \vec{h} = \vec{c}, \quad (12)$$

yields unit impulse response vectors  $\vec{h}$ , which are then  $z$ -transformed to yield the coefficients of the scattering matrix. The procedure is explained in detail in [11, 14, 18]. Until now, the transfer matrix of the heat source in a Rijke tube [11], of a straight duct [18], of a sudden change of cross-sectional area in a duct [12] and of an industrial premix swirl burner [10] have been determined with CFD/SI and successfully validated against theory, experiment or finite element calculations.

Note that it is also possible to identify the flame frequency response  $F(\omega)$  of a premix flame with CFD/SI. For system identification, the flame is considered as a SISO (single-input, single-output) element, with the velocity  $u_B$  at the burner mouth as input and the overall rate of heat  $\dot{Q}$  released by the flame as output signal, respectively, see [19]. It follows that both the scattering (or transfer) matrix of the burner as well as the frequency response function of the flame can be obtained from one single CFD run.

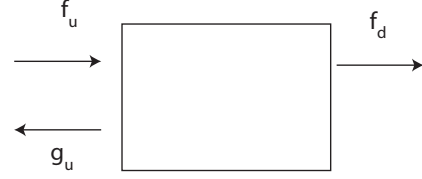


Figure 2. INCOMING WAVE AMPLITUDE  $f_u$ , TRANSMITTED AND REFLECTED SIGNALS  $f_d$  AND  $g_u$ .

### Scattering of Acoustic Energy

For vanishing mean flow Mach number, the *acoustic power*  $e$  (flux of acoustic energy) in a duct of cross sectional area  $A$  can be defined as [20]

$$e = p' u' A = \rho c (f^2 - g^2) A. \quad (\text{Units: [W]}). \quad (13)$$

Based on an acoustic energy balance between incoming and outgoing acoustic wave amplitudes, an amplification factor  $\Pi_{f_u}$  can be computed for a wave  $f_u$  traveling towards an acoustic multi-port from upstream, see Fig. 2. Making use of the scattering matrix Eqs. (5) and (6), one obtains

$$\Pi_{f_u} \equiv \left( \frac{\rho c A |f|^2|_d + \rho c A |g|^2|_u}{\rho c A |f|^2|_u} \right) = \frac{1}{\alpha \xi} |S_{11}|^2 + |S_{22}|^2, \quad (14)$$

where the area ratio  $\alpha \equiv A_u/A_d$  and the ratio of specific impedances  $\xi \equiv \rho c|_u/\rho c|_d$ .

Similarly, for a wave  $g_d$  incident on the multi-port from downstream, the energy balance leads to

$$\Pi_{g_d} \equiv |S_{12}|^2 + \alpha \xi |S_{22}|^2. \quad (15)$$

For an active element like an unsteady heat source, the amplification factor  $\Pi_{f_u}$  need not be less than unity, i.e. incoming acoustic waves can be amplified such that the emitted acoustic power exceeds the incoming power.

### RESULTS FOR A PREMIX SWIRL BURNER

The  $TD_1$  burner is a versatile premix burner with a tangential swirl generator followed by a convergent nozzle and a central lance, see Fig. 1. The length of the inlet slits of the swirl generator can be changed, thus modifying the swirl number of the flow at the burner outlet. Fuel is injected upstream of a choked cross-section to ensure perfectly premixed conditions.

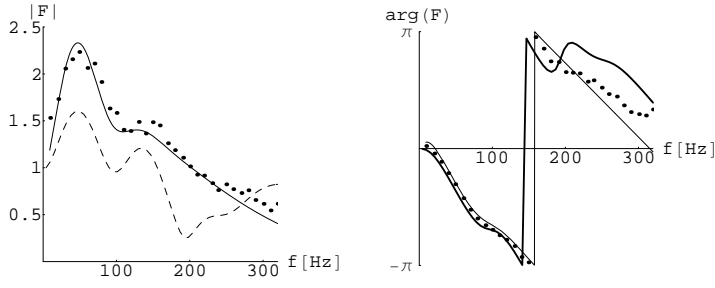


Figure 3. GAIN (LEFT) AND PHASE (RIGHT) OF FLAME FREQUENCY FUNCTION. EXPERIMENT ( $\cdot$ ), ANALYTICAL MODEL (—), CFD/SI (— —).

### Flame frequency response

Using a CTA probe to measure the velocity  $u_B$  at the burner mouth and a photomultiplier to measure the intensity of  $OH$ -chemiluminescence – which is a good measure of heat release rate  $\dot{Q}$  for a perfectly premixed flame – the flame frequency response was determined experimentally by Fischer [21]. Results are shown in Fig. 3. The configuration / operating conditions investigated are: thermal power 60 kW, equivalence ratio  $\phi = 0.75$ , swirl number  $S \approx 0.73$ , nozzle diameter 40 mm and swirler slit length 16 mm (hence "TD4016").

The flame frequency response measured by Fischer [21] can be fitted with good accuracy to the following functional form (which will prove useful in the following):

$$F(\omega) = (1+a)e^{-i\omega\tau_1 - \frac{\omega^2\sigma_1^2}{2}} - ae^{-i\omega\tau_2 - \frac{\omega^2\sigma_2^2}{2}}. \quad (16)$$

Such a formulation with two time-delays and dispersion has been proposed, e.g., in [10, 22, 23]. Using a non-linear fitting routine, the following parameter values have been determined to give good agreement with the experimental data of Fischer [21]:  $a = 0.827$ ,  $\tau_1 = 3.17$  ms,  $\sigma_1 = 0.863$  ms,  $\tau_2 = 12.4$  ms,  $\sigma_2 = 2.70$  ms, see Fig. 3.

Gentemann et al. have determined the flame frequency response of the  $TD_1$  burner with CFD/SI, using a 2-D axisymmetric, compressible URANS formulation to model the turbulent reacting flow [19]. A Reynolds-Stress turbulence model, the TFC combustion model of Zimont et al. [24] and the swirl generator model of Kiesewetter et al. [25] have been used. Further details on the computational setup, in particular the scheme for white-noise perturbation of velocity at the inlet and pressure at the outlet of the computational domain are reported in [19].

Comparing the flame frequency response determined in experiment and with CFD/SI, respectively, good quantitative agree-

ment for the phase is found up to 200 Hz, see Fig. 3. However, only rough qualitative agreement at frequencies is observed for the gain in this frequency range. It was found that the results of CFD/SI are rather sensitive to parameters of the CFD model, e.g. the thermal wall boundary condition imposed, or the *critical strain*  $g_{cr}$ , which is an important parameter of the TFC model. For the calculations reported here,  $g_{cr} = 8500$  1/s and a combustor wall temperature  $T_W = 300$  K was used. Changing to an adiabatic thermal boundary condition, much better agreement between experiment and CFD/SI was achieved (see Fig. 7 in [19]). Gentemann et al. also found that the computed spatial distribution of mean heat release is not in good agreement with the corresponding experimental results. It was concluded that a validated computational model for the  $TD_1$ -burner is required to achieve quantitative agreement also for the gain of the frequency response and for higher frequencies.

Fortunately, it turns out that the main results and conclusions of the present study do not depend in a sensitive manner on details of the flame frequency response. Therefore we proceed on the basis of the computational results of Gentemann et al.

### Scattering Matrix

In the following, results for the scattering matrix of the  $TD_1$  premix swirl burner (with combustion) are presented and discussed, see Fig. 4. It is remarkable that all four coefficients of the scattering matrix exhibit a significant peak in absolute magnitude at frequencies near 150 Hz. Before this feature is analyzed in more detail, it should be ruled out that it is due to an error in post-processing CFD or experimental data, or due to the shortcomings of the combustion model as discussed above. Therefore, it is shown that CFD/SI as well as experimental data (combined with analytical estimates for the frequency response and/or the transfer matrix of a compact burner) all give qualitatively similar results. One may conclude that the observed feature is indeed not an artifact of measurement or modelling.

...from CFD/SI Post-processing time series  $p(t)$  and  $u(t)$  at sampling planes  $u$  and  $d$  (see Fig. 1) rather than  $u_B(t)$  and  $\dot{Q}(t)$ , the scattering matrix  $\mathbf{S}$  of burner & flame can be identified from the same CFD run that was used to identify the flame frequency response  $F(f)$ . Gain and Phase of the four coefficients  $S_{ij}(f)$  are shown as continuous lines in Fig. 4.

...from experiment Using the approach proposed by Paschereit and Polifke [9], the "cold" transfer matrix of the  $TD_1$ -burner (without combustion) was determined from multi-microphone measurements with the two-source method by Fischer [21]. Unfortunately, attempts to directly measure also the "hot" transfer matrix of burner & flame (i.e. with combustion) did not yield results of satisfactory quality. However, from a

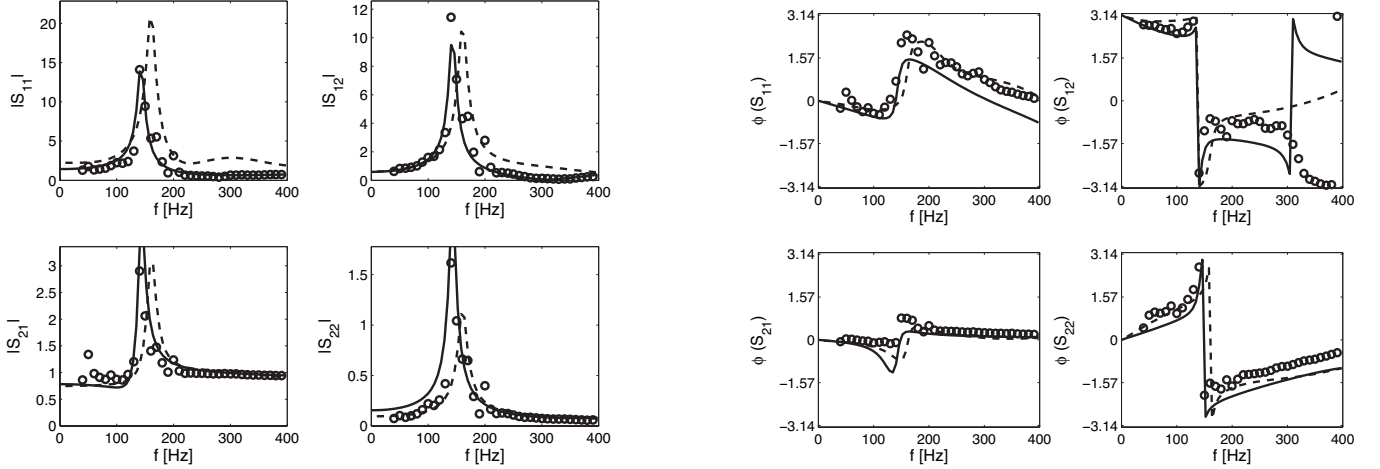


Figure 4. SCATTERING MATRIX OF BURNER & FLAME. CFD/SI (---), EXPERIMENT (O), ANALYTICAL MODEL (—).

measured frequency response  $F(\omega)$ , one can deduce a flame transfer matrix

$$\mathbf{T}_F = \begin{pmatrix} \xi & -\theta(1+F)M_h \\ -\gamma\theta M_c & 1 + \theta F(f) \end{pmatrix}, \quad (17)$$

provided that the flame is acoustically compact, and that the direct response of the heat release rate  $\dot{Q}$  to pressure perturbations  $p'$  is negligible. Here  $\theta \equiv T_h/T_c - 1$  with temperatures  $T_c = 300$  K on the cold side and  $T_h = 1523$  K on the hot side of the flame,  $M$  denotes the Mach number and  $\gamma$  is the ratio of specific heats  $c_p/c_v$ . Equation (17) is obtained by linearizing the Rankine-Hugoniot relations across a thin zone of heat release [26], a detailed derivation of this relation is given, e.g., in [5, 8].

The "hot" transfer matrix of burner & flame is computed as the matrix product of the measured cold transfer matrix of the burner  $\mathbf{T}_B$  with that of the flame according to Eq. (17),

$$\mathbf{T}_{B\&F} = \mathbf{T}_F \times \mathbf{T}_B. \quad (18)$$

The coefficients of the scattering matrix follow from Eq. (5) and are plotted in Fig. 4 (o symbols).

**An analytical model** It has been suggested that a premix swirl burner (without combustion) may be modelled as a compact acoustic element, characterized by a virtual length  $l_{\text{eff}}$ , a reduced length  $l_{\text{red}}$ , a loss coefficient  $\zeta$  and an area ratio  $\alpha$  [8, 9]. The reduced length  $l_{\text{red}}$  is often much smaller than the virtual length  $l_{\text{eff}}$  and can be neglected. At small Mach numbers, the losses are also negligible, the following expression should then serve as an analytical estimate for the "cold" burner transfer matrix (without

combustion):

$$\mathbf{T}_B \approx \begin{pmatrix} 1 - ikl_{\text{eff}} \\ 0 \quad \alpha \end{pmatrix} \quad (19)$$

with wave number  $k \equiv 2\pi f/c$ . This "cold" burner transfer matrix can again be matrix-multiplied with a transfer matrix for the flame based on the analytical estimate (16) for the flame frequency response. The resulting scattering matrix coefficients are also plotted in Fig. 4. Model parameters are:  $T_u = 300$  K,  $T_d = 1523$  K, area ratio  $\alpha = 3.4$  effective length  $l_{\text{eff}} = 1.8$  m. The last parameter was adjusted to provide best agreement with experimental results for the "cold" burner transfer matrix. Given the simplicity of the model, the agreement is surprisingly good.

To conclude, CFD/SI, experiment (combined with the linearized Rankine-Hugoniot relations for a compact flame) as well as a simple analytical model all give very similar results for the scattering matrix of the premix swirl burner investigated. One may conclude that the remarkable peaks in the absolute magnitude of all four coefficients  $|S_{ij}|$  near 150 Hz are not due to an error in the system identification process, or caused by inadequacies of the CFD model or the experimental procedure. In the following, we shall elaborate on the physical and technological significance of this feature.

### Amplification of acoustic energy

With all four coefficients of the scattering matrix  $\mathbf{S}$  larger than unity, acoustic waves incident on the burner must be strongly amplified by the unsteady combustion at frequencies around 150 Hz (note the logarithmic scale of the ordinate). Indeed, Fig. 5 shows that for the  $TD_1$  burner very significant amplification of acoustic power is observed in this frequency range.

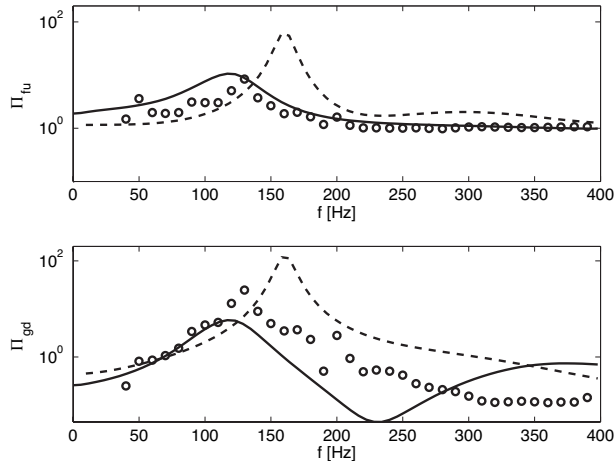


Figure 5. AMPLIFICATION FACTOR  $\Pi$  OF BURNER & FLAME FOR INCIDENT ACOUSTIC WAVE FROM UPSTREAM (TOP) AND DOWNSTREAM (BOTTOM). CFD/SI (---), EXPERIMENT (O), ANALYTICAL MODEL (—).

The graph shows results for CFD/SI, experiment [21] and the analytical model, Eq. (16), with parameters adjusted to fit the experimental data. In all three cases, the linearized Rankine-Hugoniot relations (17) were invoked to deduce a transfer matrix  $\mathbf{T}$  from the flame frequency response  $F(f)$ . Again, the agreement between computational, experimental and analytical results is not perfect – but the observed amplification is a robust qualitative feature.

The burner as such is – certainly for non-zero Mach numbers – a dissipative element, acoustic energy can only be generated by the unsteady heat release of the flame (c.f. the Rayleigh criterion). Indeed, the "cold" burner scattering matrix results in amplification factors  $\Pi$  below unity for all frequencies investigated (not shown). The flame by itself, on the other hand, does exhibit as expected amplification factors  $\Pi$  significantly larger than unity, see Fig. 6. Comparing with Fig. 5, it is seen that the maximum level of amplification is comparable to that of burner & flame. However, the location of the maximum is shifted noticeably.

## CONDITIONS FOR MAXIMUM AMPLIFICATION OF ACOUSTIC ENERGY

It has been demonstrated that the analytical model Eqs. (16), (17) and (19) reproduces the measured frequency response and scattering matrices with reasonable accuracy (with model parameters adjusted to give best agreement with experiment). Therefore, this model shall be used to analyze under which conditions significant generation of acoustic energy can occur for a premix burner.

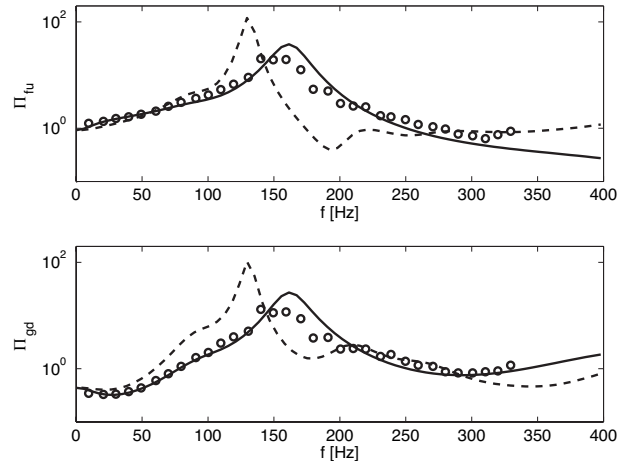


Figure 6. AMPLIFICATION FACTOR  $\Pi$  OF COMPACT FLAME FOR INCIDENT ACOUSTIC WAVE FROM UPSTREAM (TOP) AND DOWNSTREAM (BOTTOM). CFD/SI (---), EXPERIMENT (O), ANALYTICAL MODEL (—)..

The starting point is the observation that all four coefficients of the scattering matrix of the flame as well as the combined multi-port "burner & flame" are significantly larger than unity near 150 Hz – although the four coefficients of the transfer matrices show no remarkable features in this frequency range (not shown). This suggests that a small value of the denominator  $\Omega$ , which appears in the conversion from transfer to scattering matrix – see Eqs. (7) - (11) – accounts for the large scattering matrix coefficients as well as the large amplification factors  $\Pi$  observed.

In the limit of vanishing Mach numbers  $M_c, M_h \rightarrow 0$  the condition  $\Omega \approx 0$  reduces for a compact flame – see Eq. (17) – to

$$F(f) \approx -\frac{1+\xi}{\theta} = \frac{1}{1-\xi} \quad (20)$$

for an ideal gas with  $\theta = \xi^2 - 1$ . This condition is illustrated in Fig. 7, showing a polar plot of frequency responses  $F(f)$ . The point  $1/(1-\xi) \approx -0.8$  for the present conditions; it is marked with an "X" in the plot. Indeed, closest proximity to that point is observed for frequencies  $f \approx 150$  Hz. The frequency response computed with CFD/SI has a comparatively smaller gain in this frequency range and therefore comes closest to the point "X". Correspondingly, the maximum amplification predicted by CFD/SI is larger than the one obtained with the analytical model, see Fig. 6.

For the combined element "burner & flame" the condition

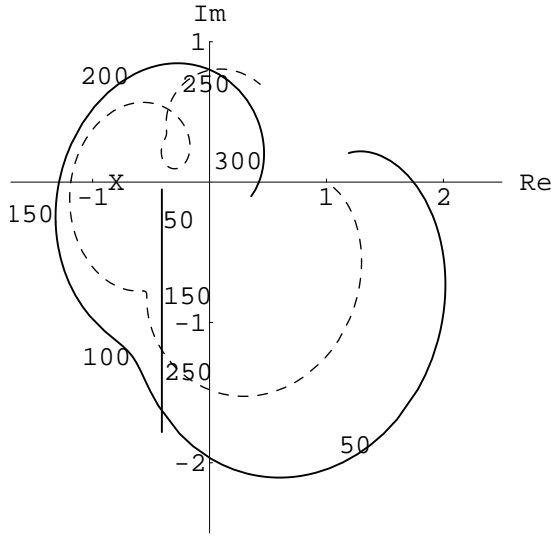


Figure 7. POLAR PLOT OF FLAME FREQUENCY RESPONSE  $F(f)$  IN THE RANGE  $f = 0 \rightarrow 320\text{Hz}$ : ANALYTICAL MODEL (—), CFD/SI (---). NUMBERS ALONG THE CURVES INDICATE THE FREQUENCIES. STRAIGHT LINE: R.H.S. OF EQ. (21).

$\Omega \approx 0$  results in the relation

$$F(f) \approx -\frac{1}{\alpha\theta} [\xi + \alpha + ik l_{\text{eff}} \xi] \quad (21)$$

in the limit of vanishing Mach numbers. Now the r.h.s of this equation (the straight vertical line in Fig. 7) exhibits a frequency dependence, strong amplification of acoustic energy occurs for those frequencies where the frequency response curve  $F(f)$  is close to that line. The plot suggest – and this is true both for the analytical model as well as CFD/SI results – that this should occur for frequencies in the range from 100 to 150 Hz, and this is indeed the behavior depicted in Fig. 5.

In concluding we remark that the burner investigated in this study exhibits, when mounted in an annular combustion chamber, a self-excited instabilities near 150 Hz for certain operating conditions [27]. Obviously, this instability frequency matches the frequency range where significant amplification of acoustic energy is predicted by our analysis.

## DISCUSSION

It is generally understood that thermo-acoustic instability will occur if two criteria are met:

1. fluctuations of pressure  $p'$  and of heat release rate  $\dot{Q}'$  are more or less in phase, such that acoustic energy is generated

by their interaction (“Rayleigh criterion”) and

2. the acoustic energy generated is larger than the amount of energy dissipated within the system or lost at the boundaries of the domain.

Therefore, comprehensive thermo-acoustic stability analysis has to take into account properties of burner & flame as well as of the combustor acoustics. Questions such as “What is a burner with favorable stability properties?” or “Which kind of burner transfer matrix yields a low Rayleigh index?” cannot be answered without also taking into consideration the environment of the burner.

The scattering matrix  $\mathbf{S}$  – and the acoustic efficiencies  $\Pi$  – on the other hand are properties of the burner “as such”, quite independent of the combustion system. And it seems justified to argue that a burner with lower acoustic efficiencies  $\Pi_{fu}$  and  $\Pi_{gd}$  will in general exhibit better stability behavior. Therefore, the analysis of the scattering matrix of burner & flame should – in addition to the transfer matrix - become one element of design for thermo-acoustic stability. In principle, it should be possible to design a burner such that time lags  $\tau_1$  and  $\tau_2$  of the flame response and the parameters  $\alpha, l_{\text{eff}}$  of the burner yield small amplification factors  $\Pi$  - at least in the vicinity of acoustic eigenfrequencies of the combustor. Even if Rayleigh’s phase criterion is met, a modest amount of damping might then be enough to stabilize combustion.

A non-trivial result of the present study is that a larger gain  $|F(f)|$  of the flame frequency response does not necessarily result in more generation of acoustic energy by the flame (or by the burner). Consideration of the “proximity plot” shown in Fig. 7 shows that there are possibly combinations of geometrical parameters  $\alpha, l_{\text{eff}}$ , operating conditions  $T_h, T_c$  and frequencies  $f$ , where a larger gain results in larger amplification factors  $\Pi$  – but indeed the opposite has been observed for the burner investigated in this study.

## ACKNOWLEDGMENT

We are indebted to A. Fischer and T. Sattelmayer for providing the experimental data. The swirl generator model of F. Kiesewetter has been used in the CFD studies. Discussions with C. Hirsch are much appreciated. Financial support by Alstom Power and Siemens Power Generation in the framework of the German AG Turbo Programme, Projects 4.4.2 and 4.4.6. is gratefully acknowledged.

## REFERENCES

- [1] Munjal, M. L., 1986. *Acoustics of Ducts and Mufflers*. John Wiley & Sons.
- [2] Keller, J. J., 1995. “Thermoacoustic Oscillations in Combustion Chambers of Gas Turbines”. *AIAA Journal*, **33**(12), pp. 2280–2287.

- [3] Bohn, D., and Deuker, E., 1993. "An acoustical model to predict combustion driven oscillations". In 20th Int'l Congress on Combustion Engines, no. **G20** in , CIMAC.
- [4] Dowling, A. P., 1995. "The calculation of thermoacoustic oscillation". *J. of Sound and Vibration*, **180**, pp. 557–581.
- [5] Polifke, W., Paschereit, C. O., and Döbbling, K., 2001. "Constructive and Destructive Interference of Acoustic and Entropy Waves in a Premixed Combustor with a Choked Exit". *Int. J. of Acoustics and Vibration*, **6**(3), pp. 135–146.
- [6] Nicoud, F., and Poinso, T., 2005. "Thermoacoustic instabilities: Should the rayleigh criterion be extended to include entropy changes?". *Combust. and Flame*, **142**(1-2), pp. 153–159.
- [7] Ibrahim, Z. M., Williams, F. A., Buckley, S. G., and Lee, J. C. Y., 2006. "An acoustic energy approach to modeling combustion oscillations". In Int'l Gas Turbine and Aeroengine Congress & Exposition, no. ASME GT2006-90956.
- [8] Polifke, W., 2004. "Combustion instabilities". In Advances in Aeroacoustics and Applications, VKI LS 2004-05, Von Karman Institute.
- [9] Paschereit, C. O., and Polifke, W., 1998. "Investigation of the Thermo-Acoustic Characteristics of a Lean Premixed Gas Turbine Burner.". In Int'l Gas Turbine and Aeroengine Congress & Exposition, no. ASME **98-GT-582**.
- [10] Schuermans, B., Bellucci, V. Guethe, F., Meili, F., Flohr, P., and Paschereit, C. O., 2004. "A detailed analysis of thermoacoustic interaction mechanisms in a turbulent premixed flame". In Int'l Gas Turbine and Aeroengine Congress & Exposition, no. ASME **GT2004-53831**.
- [11] Polifke, W., Poncet, A., Paschereit, C. O., and Döbbling, K., 2001. "Reconstruction of acoustic transfer matrices by instationary computational fluid dynamics". *J. of Sound and Vibration*, **245**(3), Aug., pp. 483–510.
- [12] Gentemann, A. M. G., Fischer, A., Evesque, S., and Polifke, W., 2003. "Acoustic transfer matrix reconstruction and analysis for ducts with sudden change of area". In 9th AIAA/CEAS Aeroacoustics Conference, AIAA.
- [13] Yuen, S. W., Gentemann, A., and Polifke, W., 2004. "Investigation of the influence of boundary conditions on system identifiability using real time system modeling". In 11th Int. Congress on Sound and Vibration (ICSV11), IIAV, pp. 3501–3508.
- [14] Polifke, W., and Gentemann, A. M. G., 2004. "Order and realizability of impulse response filters for accurate identification of acoustic multi-ports from transient CFD". *Int. J. of Acoustics and Vibration*, **9**(3), September, pp. 139–148.
- [15] Sklyarov, V. A., and Furletov, V. I., 1975. "Frequency characteristics of a laminar flame". *Plenum Publishing*(UDC 536.46:533.6.), pp. 69–77. Translated from Zhurnal Prikladnoi Mekhaniki i Tekhnicheskoi Fiziki, No. 1, pp. 84-94, Jan.-Feb. 1974.
- [16] Deuker, E., 1995. "Ein Beitrag zur Vorausberechnung des akustischen Stabilitätsverhaltens von Gasturbinen-Brennkammern mittels theoretischer und experimenteller Analyse von Brennkammerschwingungen". PhD thesis, RWTH Aachen.
- [17] Krüger, U., Hoffmann, S., Krebs, W., Judith, H., Bohn, D., and Matouschek, G., 1998. "Influence of Turbulence on the Dynamic Behaviour of Premixed Flames". In Int'l Gas Turbine and Aeroengine Congress & Exposition, Vol. ASME **98-GT-323**.
- [18] Polifke, W., 2004. "Numerical techniques for identification of acoustic multi-poles". In Advances in Aeroacoustics and Applications, VKI LS 2004-05, Von Karman Institute.
- [19] Gentemann, A., Hirsch, C., Kunze, K., Kiesewetter, F., Sattelmayer, T., and Polifke, W., 2004. "Validation of flame transfer function reconstruction for perfectly premixed swirl flames". In Int'l Gas Turbine and Aeroengine Congress & Exposition, no. ASME **GT-2004-53776**.
- [20] Morfey, C. L., 1971. "Acoustic energy in non-uniform flow". *J. of Sound and Vibration*, **14**(2), pp. 159–170.
- [21] Fischer, A., 2004. "Hybride, thermoakustische charakterisierung von drallbrennern". PhD thesis, TU-München.
- [22] Lawn, C. J., and Polifke, W., 2004. "A model for the thermo-acoustic response of a premixed swirl burner: Part II: The flame response". *Comb. Sci. Tech.*, **176**(8), August, pp. 1359 – 1390.
- [23] Hirsch, C., Fanaca, D., Reddy, P., Polifke, W., and Sattelmayer, T., 2005. "Influence of the swirler design on the flame transfer function of premixed flames". In Int'l Gas Turbine and Aeroengine Congress & Exposition, no. ASME **GT2005-68195** .
- [24] Zimont, V. L., and Lipatnikov, A. N., 1995. "A numerical model of premixed turbulent combustion of gases". *Chem. Phys. Report*, **14**(7), pp. 993–1025.
- [25] Kiesewetter, F., Hirsch, C., Fritz, J., Kröner, M., and Sattelmayer, T., 2003. "Two-dimensional flashback simulation in strongly swirling flows". *Proceedings of the ASME Turbo Expo, Atlanta, USA*, **GT2003-38395**.
- [26] Chu, B. T., 1953. "On the Generation of Pressure Waves at a Plane Flame Front". In 4th Symposium (International) on Combustion, pp. 603–612.
- [27] Kopitz, J., Huber, A., Sattelmayer, T., and Polifke, W., 2005. "Thermoacoustic stability analysis of an annular combustion chamber with acoustic low order modeling and validation against experiment". In Int'l Gas Turbine and Aeroengine Congress & Exposition, no. ASME **GT2005-68797** .